



Cite this: *RSC Adv.*, 2020, **10**, 8314

Received 31st January 2020
 Accepted 17th February 2020

DOI: 10.1039/d0ra00940g

rsc.li/rsc-advances

Direct cyanidation of silver sulfide by heterolytic C–CN bond cleavage of acetonitrile[†]

Biraj Das,^{‡,a} Pinku Saikia,^{‡,a} Mukesh Sharma,^a Manash J. Baruah,^a Subhasish Roy^b and Kusum K. Bania  ^{*,a}

Extraction of silver as silver cyanide from silver sulfide was made possible using acetonitrile as the source of cyanide. The process of cyanidation took place through the oxidation of sulfide to sulfur oxides and cleavage of the C–CN bond of acetonitrile. The reaction was found to be catalyzed by vanadium pentoxide and hydrogen peroxide. The different species involved in the cyanidation process were duly characterized using FTIR, ESI-MS, HRMS, XPS and UV-vis spectroscopic analysis. The mechanism of the cyanidation process was confirmed through *in situ* FTIR analysis.

Silver (Ag) is a precious noble metal that has found applications in photography, nanocatalysis, antibacterial agents and jewelry.^{1–3} Most importantly, it contributes to the economic growth of numerous countries. Silver metal extracted from its main ores contributes to a high percentage (~30%) of the total world production of Ag. Silver sulfide (Ag₂S) is the most common ore from which it is extracted.^{4,5} However, the traditional way of extracting Ag from Ag₂S ore has many disadvantages, as it involves the use of poisonous sodium cyanide (NaCN) or potassium cyanide (KCN), which are also used in gold (Au) extraction.^{4,5} The use of cyanide to achieve Ag leaching has led to great public concern, due to the damage it can cause to both human health and the environment. Because of the high toxicity of cyanide salts, strict regulation has been imposed to regulate or to ban the leaching of cyanide into the environment.⁶ It has been reported that the use of such cyanide salts in Au mining industries has led to the death of people working in those industries.⁷ Because of the devastating impacts of cyanide poisoning, researchers are constantly searching for alternative methods and new lixivants to replace cyanide salt in silver extraction from Ag₂S. So far, researchers have adopted various alternative methods for silver extraction, such as leaching of Ag₂S using ferricyanide-cyanide solution.^{8,9} Some have also used the precipitation method using high pressure and so on.¹⁰ Recently, the use of thiosulfate solution with buffer solution,

most commonly ammonium acetate buffer at pH = 4, has drawn great attention, and has been found to be a potential candidate for Ag extraction from its ores.¹¹ Although the method is cheaper, it consumes a high concentration of the reagent and also depends on different conditions such as pH and the kinetics of oxygen reduction.^{11,12} The reaction of silver ions (Ag⁺) with thiosulfate solution in the presence of a base (NH₃) is thermodynamically favorable, but the slow oxygen reduction process leads to deliberate leaching of Ag as silver thiosulfate complex, Ag(S₂O₃)₃⁵⁻.¹² Hence, the search for an alternative method is still an ongoing research process.

Apart from alkali cyanides, alkyl nitriles such as acetonitrile (CH₃CN) are much less toxic and can be used as a source of cyanide ions (CN⁻).¹³ However, the thermodynamic stability and high bond energy associated with the C–CN bond restrict the application of this green solvent as a source of cyanide (CN⁻) in the silver extraction process.¹⁴ Literature reports suggest that organometallic catalysts can scissor the C–CN bond very effectively.^{15–17} However, to the best of our knowledge, there is no such report that applies CH₃CN as a lixiviant in silver extraction as AgCN from Ag₂S. Recently, we reported that CH₃CN can be a suitable solvent to act as a cyanide source for the direct cyanidation of silver nitrates (AgNO₃) in the presence of vanadium pentoxide (V₂O₅) and hydrogen peroxide (H₂O₂).¹⁸ However, Ag is mostly extracted from Ag₂S in mining industries. Therefore, with our growing interest in finding a solution to replace cyanide salt, herein we demonstrate a highly effective method that allows for the direct precipitation of AgCN from Ag₂S within a very short period of time.

Initially, to achieve the cyanidation of Ag₂S and obtain silver (Ag) as silver cyanide (AgCN), silver sulfide (Ag₂S) and vanadium pentoxide (V₂O₅) were mixed in a 1 : 1 ratio using a mortar and pestle. The mixture was ground for few minutes and then dried in oven at 100 °C. The process of grinding and heating was continued for 2 h by making a paste using an ethanol/water

^aDepartment of Chemical Sciences, Tezpur University, Assam-784028, India. E-mail: kusum@tezu.ernet.in

^bDepartment of Chemistry, School of Applied Sciences, University of Science and Technology, Meghalaya, Techno City, Kling Road, Baridua 9th Mile, Ri-Bhoi, Meghalaya, India 793101

† Electronic supplementary information (ESI) available: The details material used and physical measurements, Raman spectra of V₂O₅, Ag₂S and V₂O₅–Ag₂S, XPS spectra of sulfur and the +ESI-mass spectra and HRMS. See DOI: 10.1039/d0ra00940g

‡ Both the authors contributed equally.



mixture as a solvent. The whole solid mixture was transferred to a 25 mL round bottom flask, followed by dropwise addition of 2 mL of hydrogen peroxide (30% w/v) in 10 mL CH_3CN as a solvent. The reaction mixture was then stirred for 90 min at room temperature. The solid material became completely dissolved and formed a homogeneous mixture, and the color of the solution was found to transform from black to yellow and finally to red, as shown in Scheme 1. Along with the change in color, white particles also began to precipitate from the solution, and this precipitation process was completed upon allowing the solution to stand overnight. The white precipitate was obtained by filtration using Whatmann filter paper, and was washed several times with double deionized water, and collected for further characterization. The obtained red filtrate was also kept for further analysis.

The formation of AgCN was found to be dependent on the amounts of V_2O_5 and the oxidant H_2O_2 . The optimization values for these are depicted in Tables 1 and 2. From Table 1, it was found that when 1 mmol of V_2O_5 reacted with 1 mmol of Ag_2S in presence of 2 mL of H_2O_2 in 10 mL CH_3CN , the amount of AgCN was found to be at its maximum value. On decreasing the amount of V_2O_5 , keeping all other values constant, the % yield of AgCN was found to decrease. Therefore, a 1 : 1 ratio of $\text{Ag}_2\text{S} : \text{V}_2\text{O}_5$ was considered as the optimum amount (Table 1). Similarly, from Table 2, it was ascertained that 2 mL of H_2O_2 was sufficient to give 96% of AgCN. 10 mL of CH_3CN was found to be the most appropriate amount for complete precipitation of AgCN.

The white precipitate obtained from the reaction was characterized by XRD (Fig. 1a) and FTIR (Fig. 1b) and was found to be exactly the same as that of our previous reports that confirmed the white precipitate to be silver cyanide (AgCN).^{18,19} The presence of peaks at 2θ values of 23.9, 29.8, 38.4, 49.3, 52.8, 58.5 and 61.8 confirmed the formation AgCN (Fig. 1a). The FTIR spectra also revealed the formation of AgCN with the presence of a weak vibrational band at 2166 and sharp, intense bands at 2139 cm^{-1} for $-\text{C}\equiv\text{N}$ and 476 cm^{-1} for Ag-C (Fig. 1b). The AgCN material was found to be highly pure without any contamination.

In order to investigate the role of vanadium oxide and H_2O_2 , different analyses were performed. From the XRD analysis it was evident that the 1 : 1 mixture of V_2O_5 and Ag_2S formed a composite containing the crystalline planes of both Ag_2S and V_2O_5 (Fig. 2).^{20–22} For example, the planes at 2θ values of 15.4 (200) and 20.1 (001) were present in V_2O_5 and the composite but

Table 1 Optimization of V_2O_5 using 10 mL of CH_3CN ^a

Ag_2S mg (mmol)	H_2O_2 (mL)	V_2O_5 (mg)	AgCN mg (mmol)	% Yield
247.8 (1)	2	181.8 (1)	258.6 (1.9)	96.6
	2	90.9 (0.5)	240.6 (1.8)	89.9
	2	60.6 (0.3)	230.8 (1.7)	86.2
	2	45.4 (0.25)	218.0 (1.6)	81.6

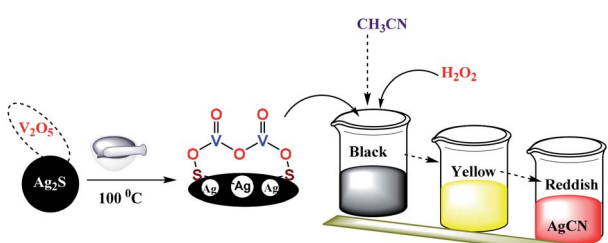
^a The values in the parentheses represent the amounts in mmol.

were absent in Ag_2S . Similarly, the planes at 2θ values of 28.9 (110), 36.7 (121) and 43.4 (202) were absent in V_2O_5 but were found in Ag_2S and the composite.^{20–22} This alternation of XRD planes clearly confirmed the good mixing of V_2O_5 with Ag_2S . The Raman spectra of Ag_2S , V_2O_5 and $\text{V}_2\text{O}_5\text{-Ag}_2\text{S}$ composite were also compared. However, the Raman signals in the $\text{V}_2\text{O}_5\text{-Ag}_2\text{S}$ composites were mostly dominated by the signals of the strong vibrational bands of V_2O_5 (Fig. S1†), as the Raman signals for Ag_2S were much weaker than those of V_2O_5 . The scanning electron microscopy (SEM) images of the composite (Fig. S2†) were also found to differ from those of Ag_2S (Fig. S3†). The elemental compositions of the composite (Fig. S4†) and Ag_2S (Fig. S5†) were assessed through energy dispersive X-ray (EDX) analysis. The presence of all the elements, *i.e.*, Ag, V, S and O, clearly revealed the formation of the composite and also the purity of the Ag_2S ore which was used as the source of silver.

FTIR analyses were performed before and after the addition of H_2O_2 (Fig. 3). When the ground mixture of Ag_2S and V_2O_5 (1 : 1) was kept at 100 °C overnight, a new band was found at 1109 cm^{-1} in the FTIR spectrum, characteristic of the S–O bond (Fig. 3a).²³ The appearance of this new band in the region of $\sim 1100\text{ cm}^{-1}$ implies the oxidation of sulfide (S^{2-}) to sulfur oxides (S_xO_y , $x = 1\text{--}2$, $y = 2\text{--}4$).²⁴ The appearance of this peak was dependent on temperature, as it was not clearly visible when the sample was treated below 100 °C (Fig. 3a). The peak was found to become more intense upon treatment with different amounts of H_2O_2 (0.5 and 1 mL), keeping the amount of CH_3CN fixed (1 mL), as shown in Fig. 3b. The conversion of S^{2-} to S_xO_y was also confirmed from the XPS analysis. The presence of S ($2\text{p}_{3/2}$) at 168.7 eV and 166.0 eV, corresponding to S_2O_3 and SO_3^{2-} ions, confirmed the oxidation of S^{2-} to S_xO_y (Fig. S6†).^{25,26} Usually, the binding energy values of sulfur (S) in sulfides are observed in the range of 162–164 eV.^{27,28} It is pertinent to mention that the oxidation of S^{2-} to S_xO_y did not happen in the absence of V_2O_5 . This clearly suggests that the

Table 2 Optimization of H_2O_2 in a 1 : 1 ratio of $\text{V}_2\text{O}_5 : \text{Ag}_2\text{S}$

V_2O_5 (mmol)	Ag_2S (mmol)	CH_3CN (mL)	H_2O_2 (mL)	% Yield AgCN
1	1	10	0.5	—
1	1	10	1	58
1	1	10	1.5	79
1	1	10	2	96



Scheme 1 Synthesis of AgCN by cyanidation of Ag_2S .



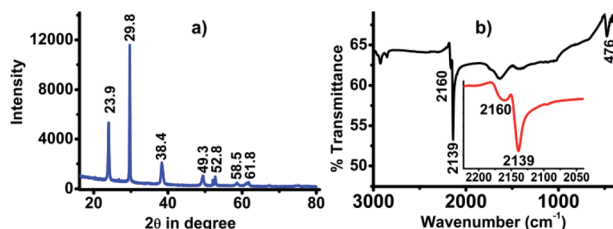
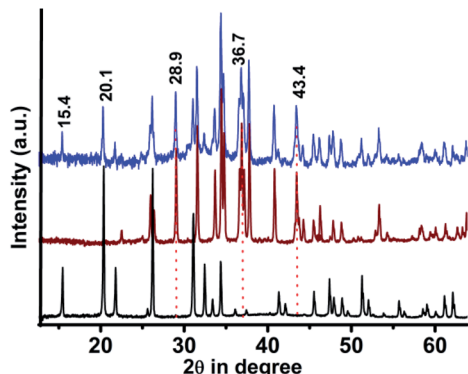
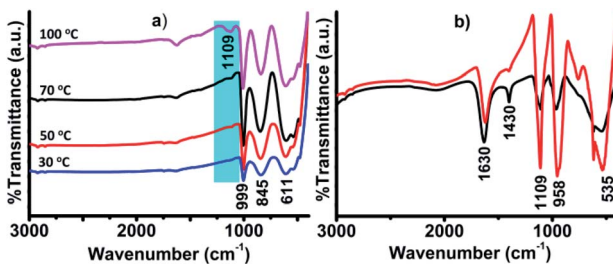


Fig. 1 (a) XRD pattern and (b) FTIR spectra of AgCN.

Fig. 2 XRD pattern of V_2O_5 (black), Ag_2S (brown) and V_2O_5 – Ag_2S composite (blue).

oxidation of S^{2-} to S_xO_y was catalyzed by V_2O_5 in the presence of H_2O_2 . Various other reports are also available in the literature supporting the oxidation of S^{2-} to S_xO_y by vanadium-oxide catalysts.^{29,30} Thus, from these analyses, it was confirmed that Ag_2S in the presence of V_2O_5 and H_2O_2 became oxidized and formed ionic silver sulfur oxide ($Ag_nS_xO_y$) compounds that easily dissociated in solution to form nAg^+ and $S_xO_y^{n-}$.

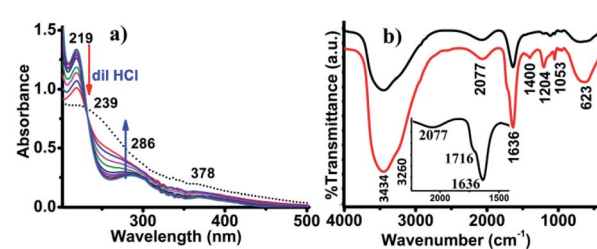
Electron Spray Ionization-Mass Spectrometry (+ESI-MS) analysis was performed to detect the formation of silver ions (Ag^+) in solution. The mass spectrum of the solution just after it became reddish in color showed a sharp intense peak with m/z values of 106.9, 109 and 148 corresponding to molecular ion peaks of Ag^+ ($m/z = 107$), its isotope ($m/z = 109$) and $[Ag(CH_3CN)]^+$ species ($m/z = 148$), as shown in Fig. S7.† The presence of an isotopic mass signal for $[Ag(CH_3CN)]^+$ was also confirmed

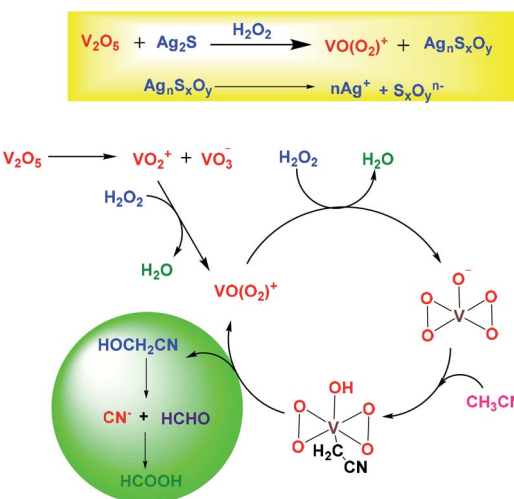
Fig. 3 (a) FTIR spectra of the composites recorded at different temperatures and (b) FTIR spectra of the composite after treating with H_2O_2 and CH_3CN ; (1 mL H_2O_2 + 1 mL CH_3CN , red line) and (0.5 mL H_2O_2 + 1 mL CH_3CN , black line).

from the High Resolution Mass Spectrometry (HRMS) analysis of the same sample showing isotopic m/z values at 148 and 150, as shown in Fig. S8.† HRMS analysis of the solution recorded after separating the $AgCN$ precipitate gave sharp signals at m/z values of 171, 153, 150 and 148, corresponding to $[OV(O_2)(H_2O)_4]^{+}$, $[OV(O_2)(H_2O)_3]^{+}$, $[^{109}Ag(CH_3CN)]^{+}$ and $[^{107}Ag(CH_3CN)]^{+}$, as shown in Fig. S9.† These m/z values for the peroxy-vanadium species were completely matched with those previously reported by Conte and his co-workers.³¹ This implied the formation of peroxy-vanadate species in solution during $AgCN$ precipitation.

The presence of peroxyvanadate species was also confirmed from the UV-vis analysis of the red solution. The UV-vis spectra presented a weak band at 378 nm due to ligand to metal charge transfer (LMCT) originating from the peroxy to vanadium ($O_2^{2-} \rightarrow V$) transition.³² As the absorption behavior of peroxyvanadate species is pH dependent,³² the UV-vis spectra were recorded with the addition of 10 μ L of 0.1 M HCl solution. After titrating with dilute HCl, two sharp new bands were observed at 219 and 286 nm. The band at 219 nm is due to the LMCT transition of $\pi_{h^*} \rightarrow d_{\sigma^*}$.³³ The band at 286 nm was attributed to the formation of $[VO(OH)]$ species resulting from the protonation of peroxyvanadate species (Fig. 4a).³⁴

Based on the above analysis, a plausible mechanism for the formation of $AgCN$ has been proposed in Scheme 2. In the presence of V_2O_5 and H_2O_2 , the Ag_2S transforms into silver sulfur oxides, as is evident from the FTIR spectroscopy. This ionic compound then becomes dissociated to release the Ag^+ . In the meantime, the CH_3CN becomes activated by the anionic yellow diperoxo species $[V(O)(O_2)_2]^-$ generated during part of the reaction (Scheme 2). The formation of diperoxo species was assumed based on the change in the color of the reaction mixture from black to yellow, and then finally to red. Further, the formation of such species was evident from UV-vis analysis (Fig. 4a). Li *et al.* also proposed the generation of such diperoxo-vanadium species upon treatment of H_2O_2 with V_2O_5 .³⁵ This anionic diperoxo species abstracts a proton from CH_3CN to form $^-\text{CH}_2\text{CN}$, which then binds to the vanadium center (Scheme 2).³⁶ A similar mechanism was also proposed by Brazdil *et al.* on the gas phase oxidation of CH_3CN at high temperature.³⁶ In the subsequent step, this $^-\text{CH}_2\text{CN}$ species gets transformed into hydroxyacetonitrile ($OH\text{CH}_2\text{CN}$) and finally produces the CN^- ion, and HCHO or HCOOH . The released CN^- ion then combines with Ag^+ to form $AgCN$. The

Fig. 4 (a) UV-vis spectra of the solution titrated against 0.1 M HCl by addition of 10 μ L at a time, and (b) *in situ* FTIR-analysis performed at 273 K (red) and 300 K (black).



Scheme 2 Plausible mechanism for CH_3CN oxidation and AgCN formation.

formation of this species was confirmed from *in situ* IR operation at 273 K where a band for surface-absorbed free CN^- ions was observed at 2077 cm^{-1} (Fig. 4b).³⁷ In addition to this, a few other peaks were also observed at 1716, 1400 and 1204 cm^{-1} corresponding to the $\text{C}=\text{O}$ vibration (inset) and the $\text{C}-\text{H}$ bending mode vibration,²³ as shown in Fig. 4b (red line). The $\text{O}-\text{H}$ vibrations were observed at 3434 and 3260 cm^{-1} . These results match well with those reported by Danger *et al.*³⁸ The appearance of these vibrational bands truly implies the oxidation of CH_3CN to formic acid *via* the formation of methanol with the liberation of CN^- . The vibrational frequency band for CN^- was clearly visible when the *in situ* operation was performed at 300 K, as the $\text{C}-\text{H}$ vibration disappeared and the $\text{C}-\text{N}$ vibration became more prominent along with the presence of the $\text{S}-\text{O}$ vibration at 1113 cm^{-1} , as shown in Fig. 4b (black line).

In summary, the long-term challenge in finding an alternative approach for the direct cyanidation of silver sulfide ore in the absence of alkali metal cyanide has been realized by using acetonitrile as the cyanide source or as a green lixiviant for the direct precipitation of silver as silver cyanide. We are currently optimizing the process towards the batch-scale production of silver cyanide from silver sulfide. We believe that the current approach offers an alternative green pathway for silver extraction.

Conflicts of interest

There are no conflicts to declare.

Acknowledgements

KKB thanks DST-SERB for financial support (SB-EMEQ-2014/463, CRG/2019/00096). BD thanks UGC-MHRD, Govt. of India, for the National Fellowship (RGNF-2017-18-SC-ASS-43132). MS also acknowledges CSIR-HRDG, New Delhi, for the SRF fellowship (No. 09/796(0097)/19-EMR-I). MJB thanks the Department of Science and Technology (DST), Govt. of India, for the DST-

INSPIRE Fellowship (No. DST/INSPIRE Fellowship/2018/IF180217).

Notes and references

- 1 S. C. Abeyweera, K. D. Rasamani and Y. Sun, *Acc. Chem. Res.*, 2017, **50**, 1754–1761.
- 2 H. L. Cao, H. B. Huang, Z. Chen, B. Karadeniz, J. Lü and R. Cao, *ACS Appl. Mater. Interfaces*, 2017, **9**, 5231–5236.
- 3 R. S. Diggikar, S. P. Deshmukh, T. S. Thopate and S. R. Kshirsagar, *ACS Omega*, 2019, **4**, 5741–5749.
- 4 G. Deschênes, J. Rajala, A. R. Pratt, H. Guo, M. Fulton and S. Mortazavi, *Miner. Metall. Process.*, 2011, **28**, 37–42.
- 5 H. Jiang, F. Xie and D. B. Dreisinger, *Hydrometallurgy*, 2015, **158**, 149–156.
- 6 M. S. Reisch, *Chem. Eng. News*, 2017, **95**, 18–19.
- 7 G. Hilson and A. J. Monhemius, *J. Cleaner Prod.*, 2006, **14**, 1158–1167.
- 8 F. Xie, D. Dreisinger and J. Lu, *Miner. Eng.*, 2008, **21**, 1109–1114.
- 9 F. Xie and B. D. Dreisinger, *Hydrometallurgy*, 2007, **88**, 98.
- 10 P. C. Holloway, K. P. Merriam and T. H. Etsell, *Hydrometallurgy*, 2004, **74**, 213–220.
- 11 S. Ayata and H. Yildiran, *Miner. Eng.*, 2005, **18**, 898–900.
- 12 Y. Cui, X. Tong and A. Lopez-Valdivieso, *Rare Met.*, 2011, **30**, 105–109.
- 13 Y. Zhu, M. Zhao, W. Lu, L. Li and Z. Shen, *Org. Lett.*, 2015, **17**, 2602–2605.
- 14 K. Zhou, C. Qin, X. L. Wang, L. K. Shao, K. Z. Yan and Z. M. Su, *CrystEngComm*, 2014, **16**, 10376–10379.
- 15 F. L. Taw, A. H. Mueller, R. G. Bergman and M. Brookhart, *J. Am. Chem. Soc.*, 2003, **125**, 9808–9813.
- 16 L. R. Guo, S. S. Bao, Y. Z. Li and L. M. Zheng, *Chem. Commun.*, 2009, 2893–2895.
- 17 F. L. Taw, P. S. White, R. G. Bergman and M. Brookhart, *J. Am. Chem. Soc.*, 2002, **124**, 4192–4193.
- 18 B. Das, M. Sharma, M. J. Baruah, K. K. Borah and K. K. Bania, *Inorg. Chim. Acta*, 2019, **498**, 119160.
- 19 B. Das, M. Sharma, C. Kashyap, A. K. Guha, A. Hazarika and K. K. Bania, *Appl. Catal., A*, 2018, **568**, 191–201.
- 20 S. Martha, D. P. Das, N. Biswal and K. M. Parida, *J. Mater. Chem.*, 2012, **22**, 10695–10703.
- 21 J. Wang, H. Feng, K. Chen, W. Fan and Q. Yang, *Dalton Trans.*, 2014, **43**, 3990–3998.
- 22 H. Li, F. Xie, W. Li, H. Yang, R. Snyders, M. Chen and W. Li, *Catal. Surv. Asia*, 2018, **22**, 156–165.
- 23 K. Nakamoto, *Infrared and Raman Spectra of Inorganic and Coordination Compounds, Part B*, John Wiley & Sons, NY, 5th edn, 1997.
- 24 L. Li, Z. Xu, A. Wimmer, Q. Tian and X. Wang, *Environ. Sci. Technol.*, 2017, **51**, 7920–7927.
- 25 R. S. C. Smart, W. M. Skinner and A. R. Gerson, *Surf. Interface Anal.*, 1999, **28**, 101–105.
- 26 H. W. Nesbitt, M. Scaini, H. Hochst, G. M. Bancroft, A. G. Schaufuss and R. Szargan, *Am. Mineral.*, 2000, **85**, 850–857.



27 B. Das, M. Sharma, A. Hazarika and K. K. Bania, *ChemistrySelect*, 2019, **4**, 7042–7050.

28 B. Das, M. J. Baruah, M. Sharma, B. Sarma, G. V. Karunakar, L. Satyanarayana, S. Roy, P. K. Bhattacharyya, K. K. Borah and K. K. Bania, *Appl. Catal., A*, 2020, **589**, 117292.

29 E. Sahle-Demessie and V. G. Devulapelli, *Appl. Catal., B*, 2008, **84**, 408–419.

30 M. D. Soriano, A. Vidal-Moya, E. N. R. I. Q. U. E. Rodríguez-Castellón, F. V. Melo, M. T. Blasco and J. L. Nieto, *Catal. Today*, 2016, **259**, 237–244.

31 (a) V. Conte, O. Bortolini, M. Carraro and S. Moro, *J. Inorg. Biochem.*, 2000, **80**, 41–49; (b) O. Bortolini, V. Conte, F. D. Furia and S. Moro, *Eur. J. Inorg. Chem.*, 1998, 1193–1197.

32 M. Kaliva, C. P. Raptopoulou, A. Terzis and A. Salifoglou, *Inorg. Chem.*, 2004, **43**, 2895–2905.

33 M. Kaliva, T. Giannadaki, A. Salifoglou, C. P. Raptopoulou, A. Terzis and V. Tangoulis, *Inorg. Chem.*, 2001, **40**, 3711–3718.

34 M. R. Maurya, S. Khurana, W. Zhang and D. Rehder, *J. Chem. Soc., Dalton Trans.*, 2002, **15**, 3015–3023.

35 C. Li, P. Zheng, J. Li, H. Zhang, Y. Cui, Q. Shao, X. Ji, J. Zhang, P. Zhao and Y. Xu, *Angew. Chem., Int. Ed.*, 2003, **42**, 5063–5066.

36 J. F. Brazdil, R. G. Teller, W. A. Marritt, L. C. Glaeser and A. M. Ebner, *J. Catal.*, 1986, **100**, 516–519.

37 S. Yoshikawa, D. H. O'Keeffe and W. S. Caughey, *J. Biol. Chem.*, 1985, **260**, 3518–3528.

38 G. Danger, A. Rimola, N. A. Mrad, F. Duvernay, G. Roussin, P. Theule and T. Chiavassa, *Phys. Chem. Chem. Phys.*, 2014, **16**, 3360–3370.

